Journal of The Electrochemical Society, **158** (9) G203-G206 (2011)
0013-4651/2011/158(9)/G203/4/$28.00 © The Electrochemical Society

Broadband Near-Infrared Luminescence from γ-ray Irradiated Bismuth-Doped Y_4GeO_8 Crystals

Beibei Xu,[a] Dezhi Tan,[a] Miaojia Guan,[a] Yu Teng,[a] Jiajia Zhou,[a] Jianrong Qiu,[a,b,z] and Zhanglian Hong[a,z]

[a]*State Key Laboratory of Silicon Materials, Zhejiang University, Hangzhou, Zhejiang 310027, P. R. China.*
[b]*State Key Laboratory of luminescence Physics and Chemistry, and Institute of Optical Communication Materials, South China University of Technology, Guangzhou, Guangdong 510640, P.R. China.*

Broadband near-infrared emission centered at 1155 nm with full width at half maximum over 300 nm has been observed in γ-ray irradiated bismuth-doped Y_4GeO_8 crystals. The luminescence was bleached completely after thermal treatment at 350°C for 2 h. Absorption spectra, electron spin resonance spectra, Raman spectra, excitation and emission spectra indicate that valence state change of bismuth was induced by γ-ray irradiation, and $^3P_1 \rightarrow {}^3P_0$ transition of Bi^+ ions is responsible for the near-infrared emission. The effect of Bi concentration on the luminescence properties of γ-ray irradiated samples was also discussed.
 [DOI: 10.1149/1.3607428]

Manuscript submitted May 11, 2011; revised manuscript received June 10, 2011. Published July 11, 2011.

Recently, Bi-doped glasses and crystals have attracted significant attention due to their ultra-broad near-infrared (NIR) luminescence in the region from 1000 to 1700 nm with full width at half maximum (FWHM) over 300 nm which covers the whole windows of optical fiber telecommunications[1,2] and the promising applications in NIR tunable lasers and superbroadband optical fiber amplifiers.[3] Up to now, NIR emission has been reported in various systems of glasses.[1–7] Very recently, broadband NIR emission has also been observed from Bi-doped crystalline SrB_4O_7, zeolites, $Ba_2P_2O_7$, BaF_2, $RbPb_2Cl_5$, sodalite, $2MgO{\cdot}2Al_2O_3{\cdot}5SiO_2$.[8–15] Most of the experimental results assigned Bi^+ as the origin of NIR emission. However, the origin of NIR emission is still in controversy, which has been ascribed to Bi^{5+},[3] the radiative e-h recombination between filled electronic configurations of $Bi^{5+}O_n^{2-}$ molecules,[7] Bi^{2+},[16] Bi^+,[1,8–13] Bi^0 (Refs. 14 and 17), Bi_2 (Refs. 18–20), Bi_2^- (Ref. 15 and 18), Bi_2^{2-} (Ref. 15) and point defects,[21] respectively.

Due to the ordered and rigid crystal lattice, it is much easier to interpret the origin of the active center in Bi-doped crystals than glasses. What's more, much higher quantum efficiency and thermal stability might be obtained in crystals than glasses. Thus study on the NIR photoluminescence properties in Bi-doped crystals can help us understand the origin of NIR luminescence and develop suitable crystalline laser materials.

In a previous work,[22] Xu et al reported NIR luminescence in γ-ray irradiated Bi-doped α-BaB_2O_4 single crystal. Under γ-ray irradiation, electrons captured by the defect centers of V''_{Ba}, which resulted from charge compensation for two Bi^{3+} substituting two Ba^{2+} ions, were released and freely drifted in the lattice. Then, Bi^{3+} which substituted Ba^{2+} in the crystal lattice captured free electrons and turned into Bi^+, resulting in NIR luminescence.

In this paper, we report on the spectroscopic properties of γ-ray irradiated Bi-doped Y_4GeO_8 crystals. Broadband luminescence at 1155 nm with FWHM over 300 nm was observed for the first time, while no apparent NIR luminescence was observed in Bi-undoped and γ-ray unirradiated Bi-doped crystals. The effect of thermal treatment and Bi concentration on the luminescence properties of γ-ray irradiated samples was also discussed. The origin of the near-infrared emission has been examined.

Experimental

Doped and un-doped samples of Y_4GeO_8 were prepared via solid state reaction. Analytical grade reagents Y_2O_3, GeO_2 and Bi_2O_3 were used as raw materials. Individual batches of 7 g were weighed according to nominal compositions $Y_{4(1-X)}GeO_8$: 4xBi (x = 0, 0.0025, 0.005, 0.0075, 0.01, 0.02, 0.03) and mixed thoroughly (in the following, all percentages are given in mol.%). Samples were synthesized in three different paths (a-c), respectively: (a) sintering at 1350°C for 4h in air; (b) after synthesized according to (a), the samples were exposed to γ-ray from a ^{60}Co source with a dose rate of 100 Gy/h for total doses of 10 kGy at room temperature; (c) the samples were synthesized according to (a) and (b), then they were thermal treated at different temperature (100, 200, 300, 350°C) in N_2 atmosphere for 2 h. Sample nomenclature is XA, XR or XRT, whereby "X" represents the concentration of Bi in mol.% (0, 0.25, 0.5, 0.75, 1.0, 2.0, 3.0), "A", "R" and "RT" mean that the samples were synthesized according to ways (a), (b) and (c), respectively, "T" is thermal treatment temperature in path (c) (T = 100, 200, 300, 350°C).

X-ray diffraction (XRD) measurements were carried out using a D/MAX-2550pc diffractometer (Rigaku International Corp., Japan) with Cu Kα as the incident radiation source. The UV-vis diffuse reflectance spectra (DRS) were recorded using a UV-3150 UV-Vis-NIR spectrophotometer (Shimadzu Corp., Japan). And they were converted into absorption spectra by K-M function

$$\frac{K}{S} = \frac{(1-R_\infty)^2}{2R_\infty} = F(R_\infty) \qquad [1]$$

where K is absorption coefficient, S is scattering coefficient and can be considered as constant, R_∞ is reflection coefficient. Infrared luminescence spectra were obtained with a ZOLIX SBP300 spectrophotometer with an InGaAs detector excited with 808 nm LD. Excitation and emission spectra in visible region were recorded using a FLS920 fluorescence spectrophotometer (Edinburgh Instrument Ltd., U.K.). Electron spin resonance (ESR) spectra were measured using a ESRA-300 Electron Paramagnetic Resonance spectrometer (Bruker Corp., Germany) operating in the X-band frequency (= 9.8655 GHz). Raman spectroscopy was performed in a Lab-RamHRUV Raman spectrograph (Jobin Yvon Corp., France) using 514.5 nm radiation from an argon ion laser for excitation. All the experiments were carried out at room temperature.

Results and Discussion

Figure 1 shows XRD patterns of $Y_{4(1-X)}GeO_8$: 4xBi, which are consistent with JCPDS card 21-1446. XRD results show the synthesized phosphors are of pure phase, which has an orthorhombic unit cell structure. No phase change occurred in the samples after γ-ray irradiation. The lattice parameters $a = 14.976$ Å, $b = 9.357$ Å, $c = 5.885$ Å, and the unit cell volume $V = 824.67$ Å^3, agree well with reported data.[23] A slight shift of the peak position for $2\theta = 29.77°$ to a smaller diffraction angle is detected from the pattern of 1A compared with that of 0.5 A (inset of Fig. 1), indicating the increase of lattice parameters with more Bi^{3+} in the crystals, confirming the assumption that some Y^{3+} ions (1.02 Å) are replaced by Bi^{3+} ions (1.17 Å).[24,25] An acceptable percentage difference in ion radii between doped and substituted ions must not exceed 30%.[26] The radius difference between the potential Bismuth species and Y^{3+} in Y_4GeO_8: Bi can be calculated from

[z] E-mail: qjr@zju.edu.cn; hong_zhanglian@zju.edu.cn

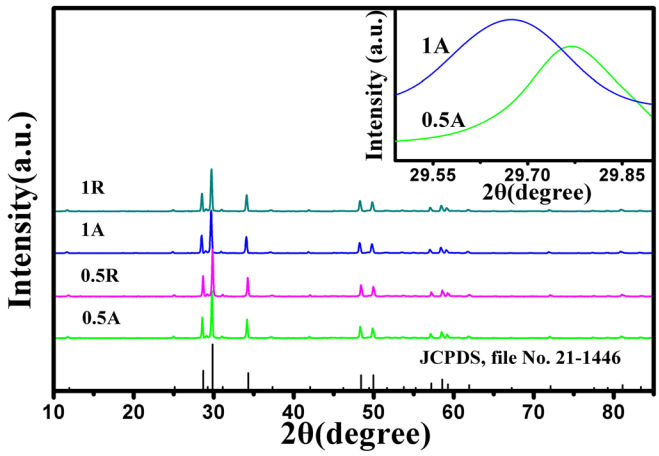

Figure 1. (Color online) XRD patterns of γ-ray unirradiated and irradiated samples (0.5A, 0.5R, 1A, 1R) and Standard JCPDS card 21-1446. The inset shows enlarged (500) diffraction peak of 0.5A and 1A.

$$D_r = 100 \times [R_m(CN) - R_d(CN)]/R_m(CN) \quad [2]$$

where D_r is the radius percentage difference, CN is the coordination number; R_m(CN) and R_d(CN) are the radius of the host cation and the dopant ion, respectively. Here, CN of Bi^{+} and Y^{3+} is taken as 8, and CN of Bi^{5+} is taken as 6, and the radius data is adopted from Refs. 8, 24, and 25. According to the size mismatch, after γ-ray irradiation, Bi^{0} ($D_r = 32.50\%$) and bismuth dimer ($D_r > 32.50\%$) can't exist in the lattice, furthermore, room temperature irradiation can't induce aggregation of previously dispersed Bi^{3+} ions isolated by oxygen ions. However, Bi^{+} ($D_r = 25.52\%$), Bi^{2+} (the radius is not available now, $D_r < 25.52\%$) and Bi^{5+} ($D_r = 27.49\%$) may exist in the lattice after γ-ray irradiation.

The absorption spectra of 0A, 0R, 1A, 1R, 1R350 are shown in Fig. 2. Peaks below 400 nm of Bi-doped samples are attributed to Bi^{3+}.[27] In the 400–700 nm wavelength range, there's no absorption in 0A and 1A, the peak at 475 nm in 0R and 1R350 may be from absorption of the generated electron and hole trap centers in the crystal matrix,[28] while strong absorption centered at 457 nm in 1R can be assigned to low-valence Bi ions[8–13] which overlays the peak at 475 nm. As the energy level of the lowest excited electronic state of Bi^{5+} (in the gas phase) is placed at 149495 cm^{-1},[17] no absorption attributed to Bi^{5+} occurs in sample 1R.

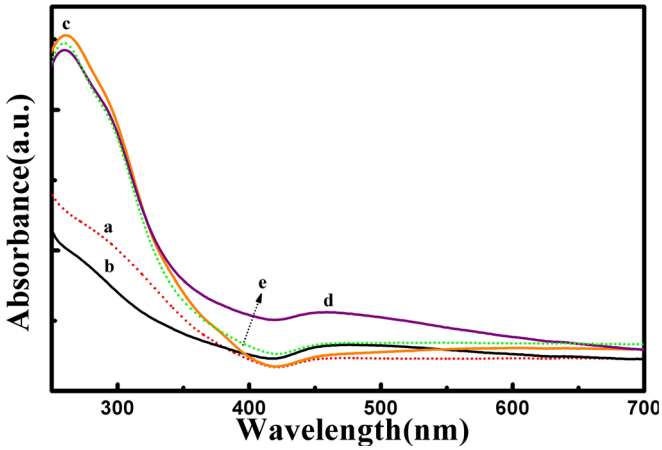

Figure 2. (Color online) Absorption spectra of γ-ray unirradiated, irradiated and heat treated samples. (a) 0A (short dot line), (b) 0R (solid line), (c) 1A (solid line), (d) 1R (solid line), (e) 1R350 (short dot line).

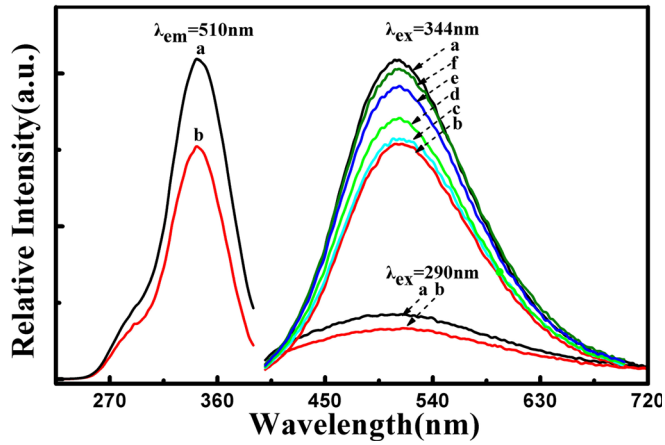

Figure 3. (Color online) Excitation ($\lambda_{em} = 510$ nm) and emission ($\lambda_{ex} = 290$, 344 nm) spectra of γ-ray unirradiated, irradiated and heat treated samples. (a) 1A, (b) 1R, (c) 1R100, (d) 1R200, (e) 1R300, (f) 1R350.

All the unirradiated Bi-doped samples exhibit turquoise luminescence. Fig. 3 shows the visible excitation and emission spectra of samples 1A, 1R, 1R100, 1R200, 1R300 and 1R350. The emission peak of sample 1A is at 510 nm, with two excitation peaks at 290 and 344 nm which are due to the electronic transition of Bi^{3+} from $^1S_0$ to $^1P_1$ (290 nm) and $^3P_1$ (344 nm), respectively.[1] Compared with the results reported by F. Zhao,[23] the excitation and emission peaks of these samples show a red shift, probably due to the different ligand field around bismuth and bismuth concentration. The luminescence intensity of 1R decreases about 26.57% compared with that of 1A, and the intensity increases as the thermal treatment temperature rises, while the luminescence intensity of 1R350 is only a little lower than that of 1A, which confirms the supposition that after γ-ray irradiation, free electrons and holes are generated in the crystals which are captured by Bi^{3+} leading to the generation of other Bi species and the decrease of emission intensity of Bi^{3+}; After thermal treatment in N_2, the free electrons and holes captured by Bi^{3+} release and recombine with each other, and finally recover to its original states, leading to the increase of Bi^{3+} and the relevant visible emission intensity.

NIR emission spectra are shown in Fig. 4. Bi-doped samples after γ-ray irradiation exhibit broad NIR photoluminescence at 1155

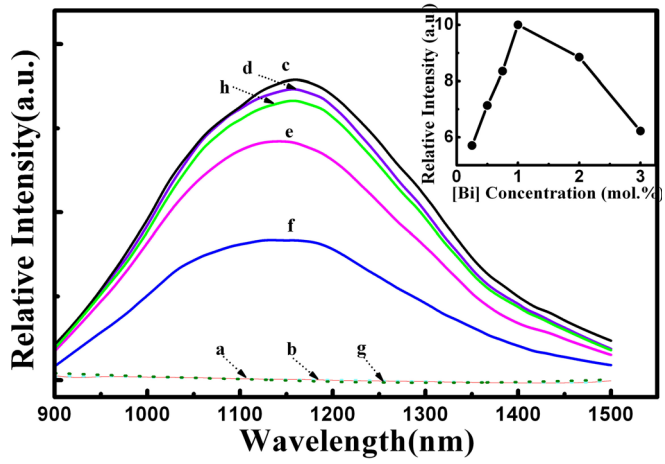

Figure 4. (Color online) NIR emission spectra of (a) 1A, (b) 0R(dot line), (c) 1R, (d) 1R100, (e) 1R200, (f) 1R300, (g) 1R350, (h) 1RL excited by 808nm LD (1RL was prepared by preserving sample 1R at room temperature in air for 2.5 months). The inset shows the relative NIR luminescence intensity as a function of x for γ-ray irradiated $(Y_{1-x}Bi_x)_4GeO_8$ ($x = 0.0025$, 0.005, 0.0075, 0.01, 0.02, 0.03) crystals excited by 808 nm LD.

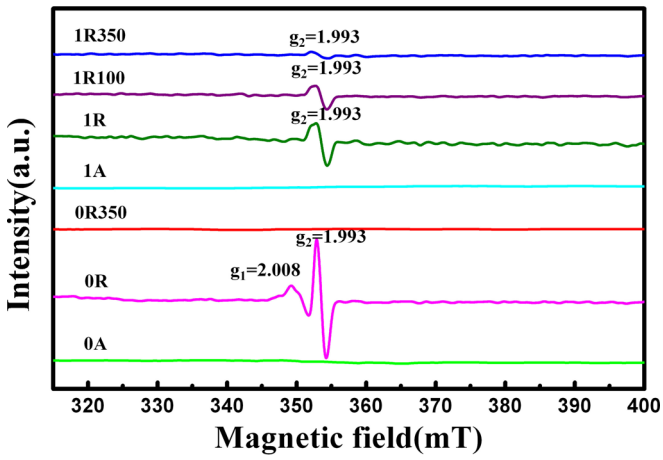

Figure 5. (Color online) ESR spectra of γ-ray unirradiated, irradiated and heat treated samples: 0A, 0R, 0R350, 1A, 1R, 1R100 and 1R350.

nm. The FWHM of sample 1R is 330 nm, which is similar to typical Bi-doped germanate glasses,[2] and wider than all Bi-doped crystals reported previously.[8–14] The peak position resembles that of other Bi-doped crystals[9,10,14] and remains unchanged with changing dopant concentration. The inset shows the relation between the emission intensity and nominal Bi concentration, maximum intensity appears at the concentration of 1 mol %. NIR emission intensity depends strongly on the thermal treatment temperature. As the temperature goes up from 100 to 350°C, the NIR emission becomes weaker and weaker and disappears at 350°C, which is consistent with the discussion in Fig. 3. There's no NIR emission in sample 0R, 1A and 1R350. Examination of the luminescence behavior of Sample 1RL shows that no apparent change was observed after preserving sample in air at room temperature for 2.5 months, indicating the γ-ray induced luminescence is stable at room temperature. Since the luminescence of Bi^{2+} is usually observed in the range of 600–700 nm,[1,27,29] and there's no NIR luminescence due to Bi^{5+} in crystals,[8–14] we suggest that the NIR luminescence may derive from Bi^{+} and is attributed to the $^3P_1 \rightarrow {}^3P_0$ transition of Bi^{+}.[9–13]

As shown in Fig. 5, no apparent electron paramagnetic resonance signal can be detected in γ-ray unirradiated samples 0A and 1A, while the γ-ray irradiated sample 0R shows signals at $g_1 = 2.008$ and $g_2 = 1.993$, which are attributed to holes and free electrons generated in the host matrix, respectively.[28,30] In the sample 1R, the signals at g_1 and g_2 vanish and decrease compared with those of undoped sample. One multivalent ion e.g. Ag^{+} can act as both electron and hole trapping center.[31] Therefore, most holes and a part of free electrons generated by the γ-ray irradiation may be captured by Bi^{3+} to form Bi^{5+} and Bi^{+}, respectively, which agrees with the valence state change of transition metal ions in glasses irradiated by femtosecond laser,[32] the process is shown in Eqs. 3 and 4

$$Bi^{3+} + 2h^{\bullet} \rightarrow Bi^{5+} \quad [3]$$

$$Bi^{3+} + 2e^{-} \rightarrow Bi^{+} \quad [4]$$

With the thermal treatment temperature rises, the holes and free electrons were released and recombined with each other, leading to the decrease of the signal intensity of g_2 and the concentration of Bi^{5+} and Bi^{+}, which is in consistent with the decrease of NIR emission intensity of the γ-ray irradiated Bi-doped samples shown in Fig. 4. In 1R350, only the signal at g_2 remains, a part of electron trapping centers still exist stably in the γ-ray irradiated Bi-doped samples due to the effect of bismuth.

The Raman spectra of the samples are presented in Fig. 6. The bands of 0A and 0R are exactly the same, indicating no molecular vibration-related structural change in the samples. The peaks centred at 515 cm^{-1} can be unambiguously attributed to the symmetric bending mode (δ_s) of Ge-O-Ge in [GeO_4] tetrahedral.[33] The band at 132 cm^{-1} is related to Ge-O-Ge vibration in [GeO_4] tetrahedral, while the rest in 0A and 0R can be assigned to Y-O-Y vibrations in [YO_8] hexahedron.[34]

By comparing the Raman spectra of 1A, 1R and 1R350 with those of 0A and 0R, one essential structure change can be observed, namely the broadening, disappearing and shift of some bands in 1A, 1R and 1R350, especially the bands related to Y-O-Y vibrations in [YO_8] hexahedron, indicating the wider distribution of the length and angle of the Y-O-Y bonds and the reduction of [YO_8] hexahedron[35] when Bi is doped. Bands at 194 cm^{-1} decreases and shifts to 191 cm^{-1}, which superposes with the band at 191 cm^{-1} for Bi^{3+} related vibrations in [BiO_6] polyhedral and the band at 203 cm^{-1} for Bi^{5+} related vibrations.[33,36,37] The band at 191 cm^{-1} is still strong in 1R350 than 1A which may be due to the existence of Bi^{5+}. The band at 592 cm^{-1} shifts to lower wavenumber at 586 cm^{-1} in 1A, 1R and 1R350. In 1A, 1R and 1R350, the bands at 140, 515 cm^{-1} are due to the symmetric stretching anion motion in angularly constrained cation-anion-cation configurations in [BiO_6] polyhedral,[36,38] which superposes with the bands at 515 and 132 cm^{-1} for [GeO_4] tetrahedral. The bands at 322, 445 and 638 cm^{-1} are assigned to the vibration of distorted [BiO_6] polyhedral[34,39]. The band at 638 cm^{-1} shifts to 633 cm^{-1} in 1R, which is due to the irradiation of γ-ray. It is interpreted that after γ-ray irradiation, some electrons escape from oxygen anions leading to the decrease of electrostatic interaction between Bi cations and O anions, which results in the increase of distance between Bi cations and O anions. The peak at 607 cm^{-1} in 1R may be related to the vibration of Bi-O^{-} bond in [BiO_6] or Bi^{5+} corresponding bond,[36,40] respectively.

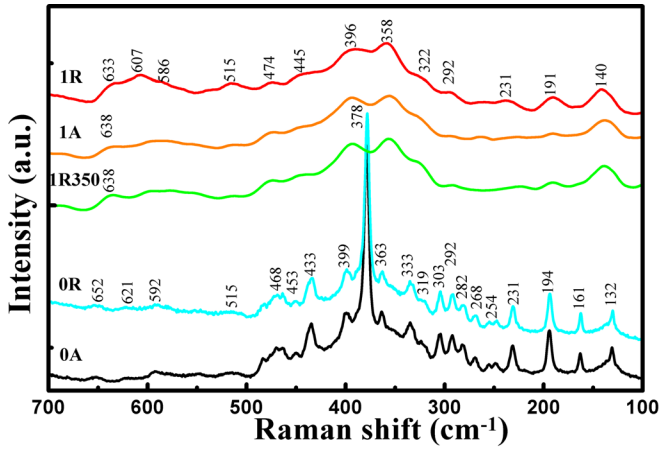

Figure 6. (Color online) Raman spectra of γ-ray unirradiated, irradiated and heat treated samples: 0A, 0R, 1A, 1R and 1R350.

Conclusion

In summary, γ-ray unirradiated Y_4GeO_8 crystal shows visible luminescence at 510 nm, while wideband NIR emission at 1155 nm with FWHM over 300 nm has been observed in Bi-doped Y_4GeO_8 crystal after γ-ray irradiation. Bi^{5+} and Bi^{+} were formed in the γ-ray irradiated crystals. The NIR luminescence is considered to be from $^3P_1 \rightarrow {}^3P_0$ transition of Bi^{+} ions. The γ-ray irradiated samples are stable at room temperature but the luminescence can be bleached at higher temperature, owing to the release of holes and free electrons from trapped center and electron-hole recombination.

Acknowledgments

This work was financially supported by the National Natural Science Foundation of China (Grant Nos. 51072054, 50872123 and

50802083) and National Basic Research Program of China (2011CB808100).

References

1. S. Zhou, N. Jiang, B. Zhu, H. Yang, S. Ye, G. Lakshminarayana, J. Hao, and J. Qiu, *Adv. Funct. Mater.*, **18**, 1407 (2008).
2. S. Zhou, H. Dong, H. Zeng, J. Hao, J. Chen, and J. Qiu, *J. Appl. Phys.*, **103**, 103532 (2008).
3. V. V. Dvoyrin, V. M. Mashinsky, L. I. Bulatov, I. A. Bufetov, A. V. Shubin, M. A. Melkumov, E. F.Kustov, E. M. Dianov, A. A. Umnikov, V. F. Khopin, et al., *Opt. Lett.*, **31**, 2966 (2006).
4. Y. Fujimoto and M. Nakatsuka, *Jpn. J. Appl. Phys. Part 2*, **40**, L279 (2001).
5. M. Peng, J. Qiu, D. Chen, X. Meng, I. Yang, X. Jiang, and C. Zhu, *Opt. Lett.*, **29**, 1998 (2004).
6. M. Peng, J. Qiu, D. Chen, X. Meng, and C. Zhu, *Opt. Lett.*, **30**, 2433 (2005).
7. I. Razdobreev, V. Yu. Ivanov, L. Bigot, M. Godlewski, and E. F. Kustov, *Opt. Lett.*, **34**, 2691 (2009).
8. L. Su, P. Zhou, J. Yu, H. Li, L. Zheng, F. Wu, Y. Yang, Q. Yang, and J. Xu, *Opt. Express*, **17**, 13554 (2009).
9. L. Su, J. Yu, P. Zhou, H. Li, L. Zheng, Y. Yang, F. Wu, H. Xia, and J. Xu, *Opt. Lett.*, **34**, 2504 (2009).
10. H. Sun, A. Hosokawa, Y. Miwa, F. Shimaoka, M. Fujii, M. Mizuhata, S. Hayashi, and S. Deki, *Adv. Mater.*, **21**, 3694 (2009).
11. J. Ruan, L. Su, J. Qiu, D. Chen, and J. Xu, *Opt. Express*, **17**, 5163 (2009).
12. A. G. Okhrimchuk, L. N. Butvina, E. M. Dianov, N. V. Lichkova, V. N. Zagorodnev, and K. N. Boldyrev, *Opt. Lett.*, **33**, 2182 (2008).
13. H. Sun, M. Fujii, Y. Sakka, Z. Bai, N. Shirahata, L. Zhang, Y. Miwa, and H. Gao, *Opt. Lett.*, **35**, 1743 (2010).
14. M. Peng, B. Sprenger, M. A. Schmidt, H. G. L. Schwefel, and L. Wondraczek, *Opt. Express*, **18**, 12852 (2010).
15. V. O. Sokolov, V. G. Plotnichenko, and E. M. Dianov, *Opt. Lett.*, **33**, 1488 (2008).
16. E. M. Dianov, *Quantum Electron.*, **40**, 283 (2010).
17. C. Moore, *Atomic Energy Levels Nat. Bur. Stand.*, p. 219, US Government Printing and Publishing Office, Washington, DC (1971).
18. S. Khonthon, S. Morimoto, Y. Arai, and Y. Ohishi, *J. Ceram. Soc. Jpn.*, **115**, 259 (2007).
19. B. Denker, B. Galagan, V. Osiko, I. Shulman, S. Sverchkov, and E. Dianov, *Appl. Phys. B*, **95**, 801 (2009).
20. M. Hughes, T. Suzuki, and Y. Ohishi, *Opt. Mater.*, **32**, 368 (2009).
21. M. Y. Sharonov, A. B. Bykov, V. Petricevic, and R. R. Alfano, *Opt. Lett.*, **33**, 2131 (2008).
22. J. Xu, H. Zhao, L. Su, J. Yu, P. Zhou, H. Tang, L. Zheng, and H. Li, *Opt. Express*, **18**, 3385 (2010).
23. F. Zhao, P. Guo, G. Li, F. Liao, S. Tian, and X. Jing, *Mater. Res. Bull.*, **38**, 931 (2003)
24. R. D. Shannon, *Acta Crystallogr. Sect. A*, **32**, 751 (1976).
25. J. Slater, *Quantum Theory of Molecules and Solids, Symmetry and Energy Bands in Crystals*, p. 55, McGraw-Hill, New York (1965).
26. M. Peng, Z. Pei, G. Hong, and Q. Su, *J. Mater. Chem.*, **13**, 1202 (2003).
27. G. Blasse, A. Meijerink, M. Nomes, and J. Zuidema, *J. Phys. Chem. Solids*, **55**, 171 (1994).
28. S. F. Zhou, W. Lei, J. Chen, J. Hao, H. Zeng, and J. Qiu, *IEEE Photonics Technol. Lett.*, **21**, 386 (2009).
29. M. Peng, N. Da, S. Krolikowski, A. Stiegelschmitt, and L. Wondraczek, *Opt. Express*, **17**, 21169 (2009).
30. J. W. H. Schreurs, *J. Chem. Phys.*, **47**, 818 (1967).
31. Q. Zhao, J. Qiu, X. Jiang, C. Zhao, and C. Zhu, *Opt. Express*, **12**, 4035 (2004).
32. J. Qiu, C. Zhu, T. Nakaya, J. Si, K. Kojima, F. Ogura, and K. Hirao, *Appl. Phys. Lett.*, **79**, 3567 (2001).
33. E. J. Baran and C. Cascales, *J. Raman Spectrosc.*, **33**, 838 (2002).
34. RASMIN Web: http://riodb.ibase.aist.go.jp/db092/cgi-bin/inorganic_search.pl?lang=E&name=&Atom_O=ON&Atom_Y=ON
35. V. O. Sokolov, V. G. Plotnichenko, V. V. Koltashev, and E. M. Dianov, *J. Phys. D: Appl. Phys.*, **42**, 095410 (2009).
36. A. Dias and R. L. Moreira, *J. Raman Spectrosc.*, **41**, 698 (2010).
37. V. N. Denisov, A. N. Ivlev, A. S. Lipin, B. N. Mavrin, and V. G. Orlov, *J. Phys.: Condens. Matter*, **9**, 4967 (1997).
38. R. J. Betsch and W. B. White, *Spectrochim. Acta A*, **34**, 505 (1978).
39. L. Baia, T. Iliescu, S. Simon, and W. Kiefer, *J. Mol. Struct.*, **599**, 9 (2001).
40. S. Venugopalan and K. Ramdas, *Phys. Rev. B*, **5**, 4065 (1972).